ELSEVIER

International Journal of Biological Macromolecules
18 (1996) 101–114

INTERNATIONAL JOURNAL OF
Biological
Macromolecules
STRUCTURE, FUNCTION AND INTERACTIONS

Molecular dynamics simulations of hybrid and complex type oligosaccharides

P.V. Balaji, P.K. Qasba*, V.S.R. Rao

Laboratory of Mathematical Biology, National Cancer Institute, National Institutes of Health, Building Park 5, Room 410, 12420 Parklawn Drive MSC 8105, Bethesda, MD 20892-8105, USA

Received 20 June 1995; revision received 7 July 1995; accepted 12 July 1995

Abstract

Conformational preferences of hybrid ($GlcNAc_1Man_5GlcNAc_2$) and complex ($GlcNAc_1Man_3GlcNAc_2$; $GlcNAc_2Man_3GlcNAc_2$) type asparagine-linked oligosaccharides and the corresponding bisected oligosaccharides have been studied by molecular dynamics simulations for 2.5 ns. The fluctuations of the core Man-α1,3-Man fragment are restricted to a region around (−30°,−30°) due to a 'face-to-face' arrangement of bisecting GlcNAc and the β1,2-GlcNAc on the 1,3-arm. However, conformations where such a 'face-to-face' arrangement is disrupted are also accessed occasionally. The orientation of the 1,6-arm is affected not only by changes in χ, but also by changes in Φ and Ψ around the core Man-α1,6-Man linkage. The conformation around the core Man-α1,6-Man linkage is different in the hybrid and the two complex types suggesting that the preferred values of Φ,Ψ, and χ are affected by the addition or deletion of saccharides to the α1,6-linked mannose. The conformational data are in agreement with the available experimental studies and also explain the branch specificity of galactosyltransferases.

Keywords: Carbohydrates; Conformation; Asn-linked oligosaccharide; Hybrid type; Complex type; Oligosaccharide processing

1. Introduction

Glycoproteins constitute a class of biopolymers differing from proteins by the presence of oligosaccharides covalently linked to the polypeptide chain through the side chain of Asn or Ser/Thr. Studies on animal and plant cell glycoproteins have revealed a variety of structurally different oligosaccharides which are responsible for the diversity in their biological functions such as cellular recognition, cellular adhesion, protein targeting, etc. The carbohydrate moieties are generally branched and differ both in the nature of the saccharide residues and the type of linkages. *N*-Linked oligosaccharides contain a common pentasaccharide core Man-α1,6[Man-α1,3]-Man-β1,4-GlcNAc-β1,4-GlcNAc-β1,- to which different saccharides are added to give oligosaccharides with different specificities.

During the biosynthesis of the Asn-linked glycoproteins, the $Glc_3Man_9GlcNAc_2$ precursor is co-translationally transferred from the dolichol pyrophosphate donor to the side chain of Asn residue at the glycosylation site [1]. In the early processing stage, the precursor oligosaccharide is subjected to trimming of saccharides (from $Glc_3Man_9GlcNAc_2$ to $Man_5GlcNAc_2$) by a number of glycosidases in the ER, transitional ER and the *cis*-Golgi apparatus [2]. Middle stage processing occurs in both the *cis*- and the *medial*-Golgi apparatus wherein the oligosaccharide is subjected to the action of α-mannosidase(s) II and *N*-acetylglucosaminyltransferases (GlcNAc-T) for elongation. The action of GlcNAc-T I is a prerequisite for the action of α-mannosidase(s) II and other enzymes like GlcNAc-T II, III and IV. On the other hand, the addition of bisecting *N*-acetylglucosamine (bis-GlcNAc) by GlcNAc-T III prevents the action of some of the glycosyltransferases resulting in bisected hybrid/complex oligosaccharides [3]. The late-stage processing occurs largely in the *trans*-Golgi apparatus where the Asn-linked oligosaccharides are elongated by the action of several glycosyltransferases

* Corresponding authorTel.: 301 496 1365; Fax: 301 402 0690; e-mail: qasba@helix.nih.gov.

SSDI 0141-8130(95)01064-2

[4]. Although the assembly of these oligosaccharides on proteins occurs in closely related pathways in many organisms, the exact processing depends on the species, tissue, developmental stage, and the tertiary structure of the protein and is controlled by the specificities of the processing enzymes [5]. Alterations in the activities of several glycosyltransferases have been associated with cellular dysfunctions [6–16].

A knowledge of the 3-dimensional structure of both the *N*-linked oligosaccharides and the glycosyltransferases and glycosidases will be very useful in understanding the biosynthesis and the function of glycoproteins. However, no information is available about the 3-dimensional structure of these enzymes and most of the studies have so far been limited to computer modelling and NMR studies of oligosaccharides [17–25]. This includes the high mannose, hybrid and complex type of Asn-linked oligosaccharides and the intermediates that occur during their biosynthesis. The conformational preferences of the high mannose oligosaccharides derived from the recent MD simulation study [25] were found to be in qualitative agreement with the experimental observations and the data were used to rationalize some of the biochemical results [26]. The MD simulations have now been extended to the conformational analysis of some asparagine-linked oligosaccharides that are both found on glycoproteins and are early intermediates in the biosynthesis of other hybrid and complex type oligosaccharides (Fig. 1).

2. Methods

2.1. Generation of coordinates

Φ,Ψ in 1,2-, 1,3- and 1,4-linkages are defined as H1-C1-O-CX and C1-O-CX-HX, where CX and HX are the aglyconic atoms. Φ,Ψ,χ in 1,6-linkage are defined as H1-C1-O-C6, C1-O-C6-C5, and O-C6-C5-H5, respectively (Fig. 2a). The coordinates were generated using the in-house software package *IMPAC* (Interactive Modeling Package for Carbohydrates) developed by P. Sailaja, P.V. Balaji, B. Vijaya Sai Reddy and V.S.R. Rao at the Molecular Biophysics Unit, Indian Institute of Science,

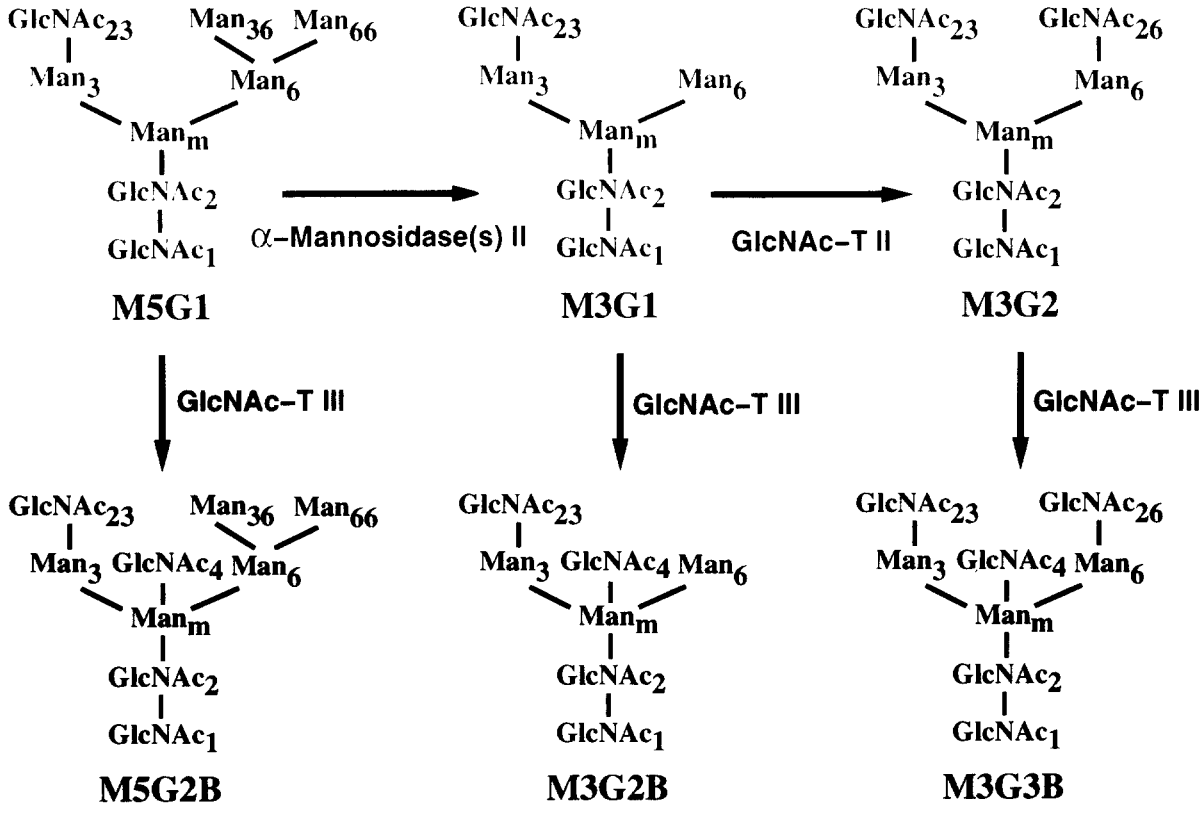

Fig. 1. Structures of the hybrid and complex type Asn-linked oligosaccharides studied by molecular dynamics simulations. The numbers associated with the individual monosaccharide residues are explained in Fig. 2. $GlcNAc_4$ and bis-GlcNAc are used interchangeably to refer to the bisecting GlcNAc. Each oligosaccharide is named by the total number of mannose and *N*-acetylglucosamine residues (excluding the core chitobiose residues, $GlcNAc_1$ and $GlcNAc_2$) present in it (MnGn). The alphabet 'B' is added at the end of the name to indicate the presence of bisecting GlcNAc (MnGnB). M5G1 and M5G2B are also referred to as hybrid oligosaccharides and M3G1, M3G2B, M3G2 and M3G3B as complex oligosaccharides. The synthesis of M3G2 by the sequential action of α-mannosidase(s) II and GlcNAc-T II on M5G1 through the intermediate formation of M3G1 is shown by arrows. Action of GlcNAc-T III on any of these 3 oligosaccharides leads to the formation of the corresponding bisected structure.

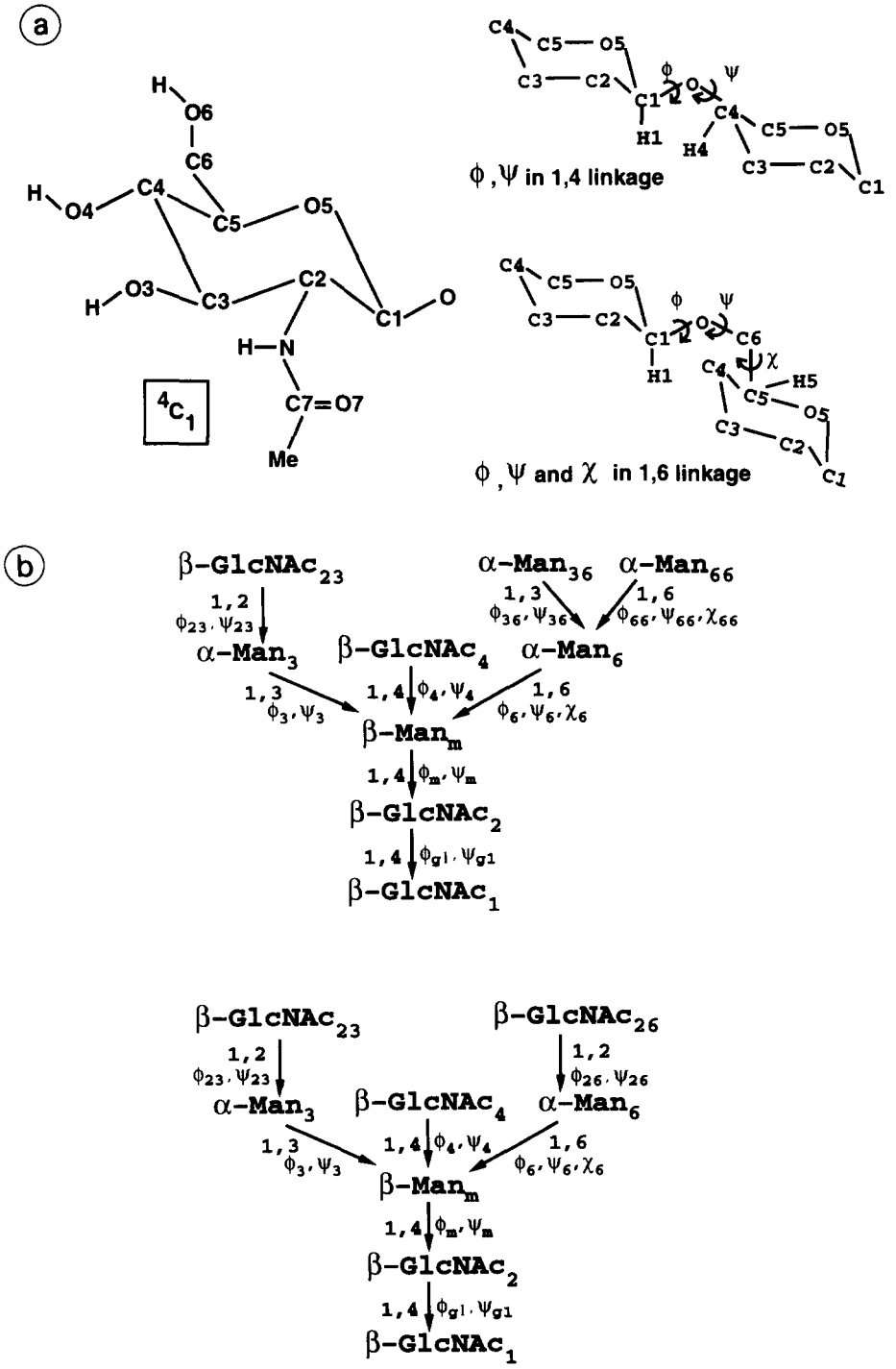

Fig. 2. (a) Schematic diagram showing the atom names and torsion angle definition used in the present study. All the saccharides are $^4C_1$(D) pyranosides. Φ,Ψ in 1,2- and 1,3-linkages are defined in the same way as in 1,4-linkage. (b) Nomenclature used for identifying saccharide residues. The middle mannose residue β1,4-linked to the core chitobiose (GlcNAc$_2$–β1,4-GlcNAc$_1$) is termed Man$_m$. Mannoses α1,3- and α1,6-linked to Man$_m$ are denoted as Man$_3$ and Man$_6$, respectively, where the subscripts 3 and 6 denote the type of linkage. Since all the glycosidic linkages (1,2-, 1,3-, 1,4- and 1,6-) are through C1, 1 is omitted in the numbering scheme and only the position (i.e., 2, 3, 4, or 6) of the second saccharide is used to denote the type of linkage. For the remaining saccharides, the first number in the suffix denotes the linkage through which it is linked to the preceding saccharide. Numerals following the first number indicate how the preceding residue is linked up to the branch point (Man$_m$). Hence the last numeral also indicates the branch on which the residue is present. For example, Man$_{36}$ is 1,3-linked to the previous mannose Man$_6$ which constitutes the 1,6-branch. The torsion angles are given the same subscript as the monosaccharide whose anomeric carbon is involved in the glycosidic linkage.

Bangalore. Initial torsion angles around the interglycosidic bonds were taken from the disaccharide Φ,Ψ maps [27,28] and energy minimization studies [29,30] and are 60°,0° for β1,4-, −30° to −50°,−20° to 50° for α1,3-, and −30° to −60°, −40° to 20° for the β1,2-linkages. The stereochemically allowed region in the Φ,Ψ map of all these 3 linkages were reasonably well sampled during the simulations (see Results) and hence other initial conformations were not considered. In the case of the core α1,6-linkage, simulations were initiated with at least 2 χ_6 values (180° and −60°; see Fig. 2b for torsion angle nomenclature) for all the oligosaccharides. However, only one initial conformation was found to be sufficient for Φ_{66},Ψ_{66},χ_{66}.

2.2. Calculation procedure

All the calculations were performed using Biosym's InsightII/Discover (versions 2.3.5/2.9) on National Cancer Institute's Cray Y-MP 8D/8128 supercomputer located at the Frederick Cancer Research and Development Center and in essentially the same way as described earlier [25,26,31,32]. Briefly, the initial coordinates obtained from IMPAC were first minimized by Newton-Raphson algorithm till the maximum derivative is less than 0.001 kcal/mol/Å. This was followed by an equilibration period of 40 ps and a productive run of 2500 ps at a constant temperature of 300°K. The average temperature in all the simulations was maintained at 300°K with a standard deviation of up to ±12° in various simulations. A time step of 1 fs was used for integration which was done using Verlet's leap frog algorithm. Simulations were also done with different seed values for the random number generator so that different initial velocities are assigned and different conformations are generated from the same initial conformation. Coordinate information was stored for every 500 steps and only the trajectory data from the productive run were considered for analysis.

MD simulations of the disaccharide Man-α1,3-Man were carried out with the CVFF force field of Discover and the theoretical NOE values back-calculated using this trajectory information were found to be in good agreement with the experimental values [32]. Conformations of oligosaccharides derived from earlier MD simulations carried out using CVFF force field were found to be in qualitative agreement with the experimental observations [26] and hence, for the present simulations also, CVFF force field was used. No explicit hydrogen bonding term was included in the calculations. Interactions between all the nonbonded atom pairs were calculated without any distance cutoffs. A distance dependent dielectric constant of 4.0*r was used for calculating the electrostatic interactions.

3. Results

3.1. β1,4-Linkages

The MD simulations of all the oligosaccharides studied here (Fig. 1) show that the fluctuations in Ψ_{gl} are more restricted than Φ_{gl} and are around 0°. Φ_{gl}

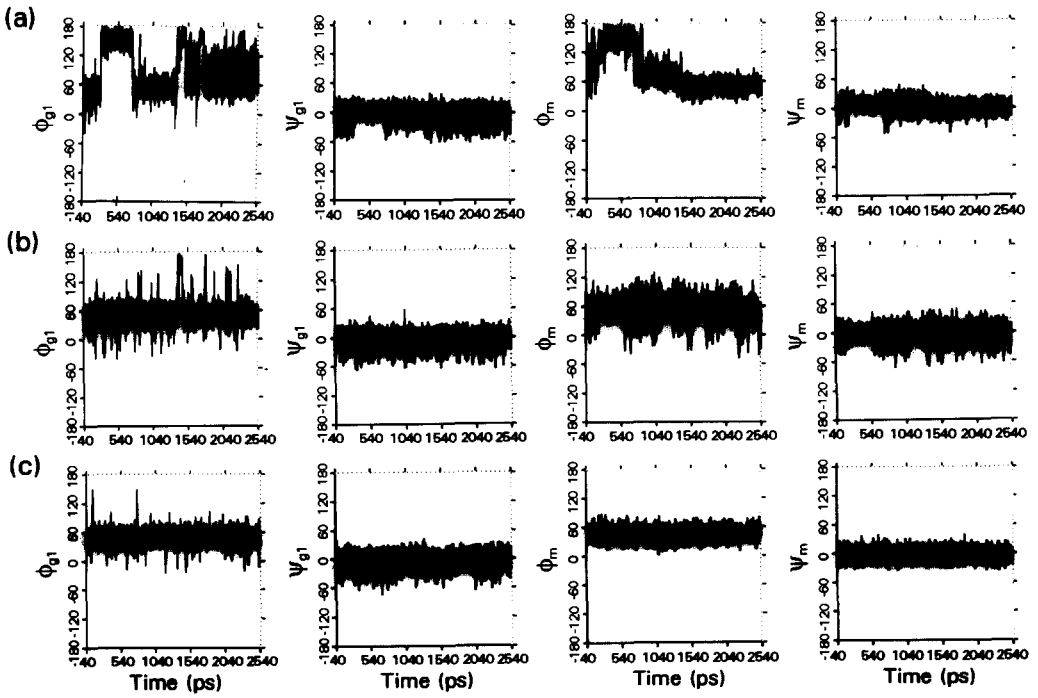

Fig. 3. Variation of the interglycosidic torsion angles around the core β1,4-linkages. Plots of Φ_{gl},Ψ_{gl} and Φ_m,Ψ_m as a function of time obtained from the dynamics trajectories of the oligosaccharides M5G2B (a), M3G1 (b) and M3G3B (c). The plots for M5G1, M3G2B and M3G2 are similar to that of M5G2B, M3G1 and M3G3B, respectively, and hence are not shown in the figure.

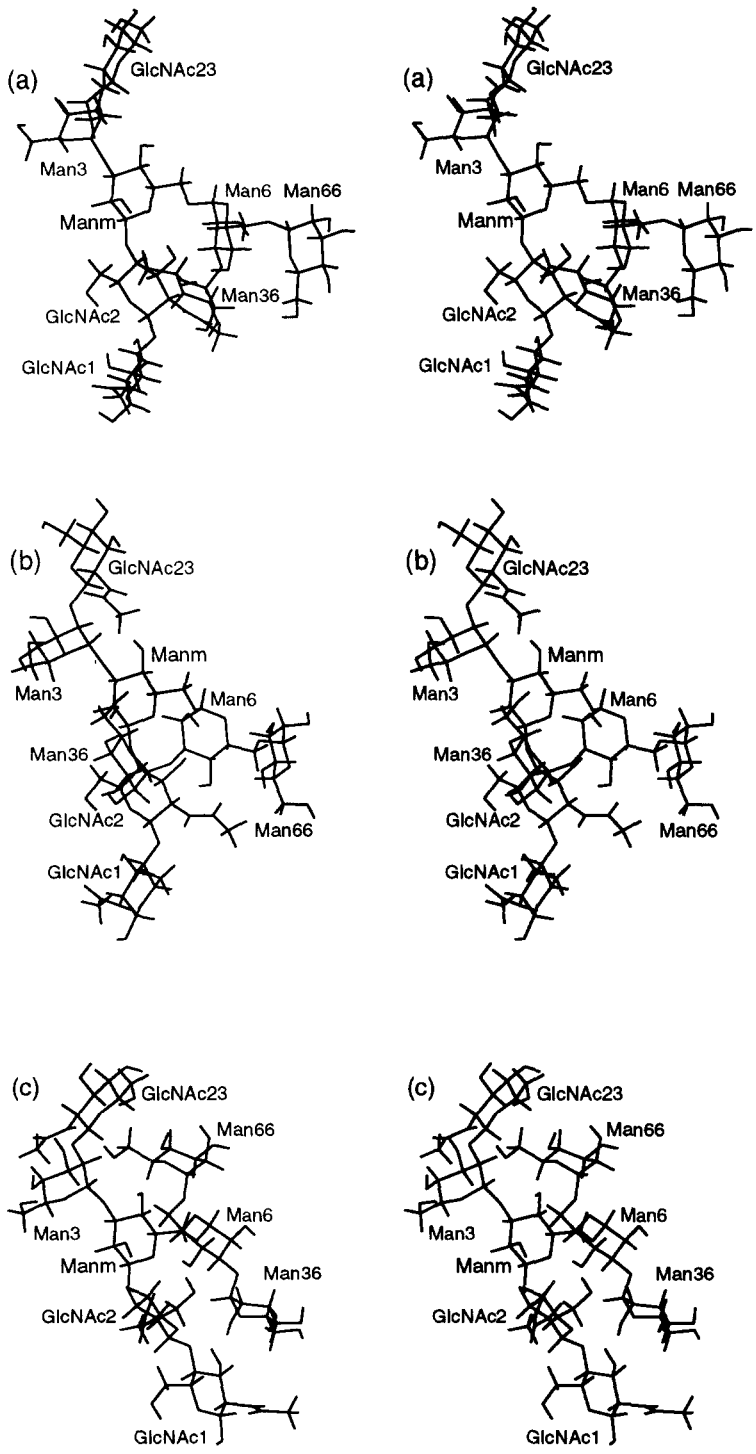

Fig. 4. Stereo diagrams of 3 conformers of the hybrid oligosaccharide M5G1 accessed during the MD simulations to show the changes in Φ_m associated with the changes in χ_6. The 3 conformers were accessed during the MD simulations at 1260 ps (a) and 784.5 ps (b) (initial Φ_6,Ψ_6,χ_6 = −60°,150°,−60°) and 456 ps (c) (initial Φ_6,Ψ_6,χ_6 = −60°,150°,180°). The Φ_6,Ψ_6,χ_6 and Φ_m,Ψ_m values in the 3 conformers are −41°,176°,−69° and 57°,4° (a), 30°,102°,−69° and 48°,12° (b) and −39°,−111°,−153° and 143°,16° (c). Notice the change in the conformation of the oligosaccharide around the Man_m–β1,4-$GlcNAc_2$ fragment in conformer (c) compared to that in (a) and (b). The conformer (c) is accessed only for a short period during the beginning of the MD simulation run. The changes in the orientation of the 1,6-arm brought about by changing Ψ_6 alone ((a) and (b) compared with (c)) and by changing only Φ_6 and Ψ_6 ((a) and (b)) are also illustrated. To avoid spurious differences in the orientations, the 3 conformers were first superimposed over each other with the C1, C3 and C5 atoms of Man_m as reference points and separated subsequently.

fluctuates around 65° in the hybrid oligosaccharides and around 45° in the complex oligosaccharides (Fig. 3) suggesting that the preferred value of Φ_{gl} is influenced by Man_{36} and Man_{66}. However, bis-GlcNAc does not show any direct effect on the core chitobiose conformation. Hybrid oligosaccharides access conformations in the range Φ_{gl} = 140–180° more frequently than complex oligosaccharides (Fig. 3a compared with Fig. 3b,c). Φ_m,Ψ_m fluctuate around 55°,0 in all the oligosaccharides (Fig. 3). In some simulations of unbisected and bisected hybrid oligosaccharides, Φ_m initially fluctuates around 140° and then changes to 60° (Fig. 3a; M5G2B) leading to flipping of chitobiose relative to rest of the oligosaccharide. This transition of Φ_m from around 140° to around 60° is correlated with the change in χ_6 (Fig. 4). In M3G1 and M3G2B, Φ_m fluctuates more than Ψ_m (Fig. 3b; M3G1). In all the 3 bisected oligosaccharides M5G2B, M3G2B and M3G3B, Φ_4,Ψ_4 favor values around 60°,10° (data not shown) and the fluctuations in these angles are similar to those observed in the hexasaccharide Man-α1,6[Man-α1,3][GlcNAc-β1,4]-Man-β1,4-GlcNAc-β1,4-GlcNAc (i.e., same as M3G2B but without $GlcNAc_{23}$) [32]. This suggests that bis-GlcNAc has relatively less flexibility and the conformational behavior of the $GlcNAc_4$–β1,4-Man_m fragment is not affected by $GlcNAc_{23}$.

3.2. α1,3-Linkages

In the unbisected hybrid (M5G1) and complex (M3G1 and M3G2) oligosaccharides, Φ_3 fluctuates from −60° to 0° and Ψ_3 from −60° to 60°; however, Φ_3 shows frequent transitions to values between 0 and 60° (Fig. 5a; M5G1). On the other hand, the fluctuations of Φ_3 (−60° to −5°) and Ψ_3 (−30 to 20°) are restricted in the bisected hybrid (Fig. 5b; M5G2B) and complex (Fig. 5c; M3G3B) oligosaccharides although Φ_3 shows occasional transitions to around 60° in M3G3B. This suggests that the fluctuations in Φ_3,Ψ_3 are restricted to a narrow range by bis-GlcNAc and that the removal of Man_{36} and Man_{66} by α-mannosidase(s) II does not significantly affect either the preferred conformations or the flexibility of Man_3–α1,3-Man_m fragment. The dampening effect of bis-GlcNAc on Man_3–α1,3-Man_m has been inferred from NMR studies also [33]. In hybrid oligosaccharides, Φ_{36},Ψ_{36} around the Man_{36}–α1,3-Man_6 linkage fluctuate around −40°,10° (Fig. 5d,e) as in the high mannose oligosaccharides [25].

MD simulations of the disaccharide Man-α1,3-Man and the hexasaccharide Man-α1,6[Man-α1,3][GlcNAc-β1,4]-Man-β1,4-GlcNAc-β1,4-GlcNAc (i.e., core pentasaccharide with a bisecting GlcNAc) have been reported recently [32]. The fluctuations of Φ_3,Ψ_3 around the Man_3–α1,3-Man_m fragment in this hexasaccharide were found to be very similar to those of Φ,Ψ in the Man-α1,3-Man disaccharide implying that the bis-GlcNAc has no dampening effect on the core α1,3 linkage in this hexasaccharide. However, the fluctuations of Φ_3,Ψ_3 are dampened in M5G2B (Fig. 5b), M3G2B, and M3G3B (Fig. 5c) suggesting that the bis-GlcNAc has a dampening effect on the Man_3–α1,3-Man_m fragment only when $GlcNAc_{23}$ is linked to Man_3. In the preferred conformations of M3G3B, bis-GlcNAc ($GlcNAc_4$) and $GlcNAc_{23}$ are positioned 'face-to-face' which probably stabilizes this conformation (Fig. 6a). Such a 'face-to-face' arrangement of $GlcNAc_{23}$ and $GlcNAc_4$ has been inferred from NMR studies also [33–35]. However, conformations wherein such 'face-to-face' arrangement of $GlcNAc_4$ and $GlcNAc_{23}$ are disrupted by a change in

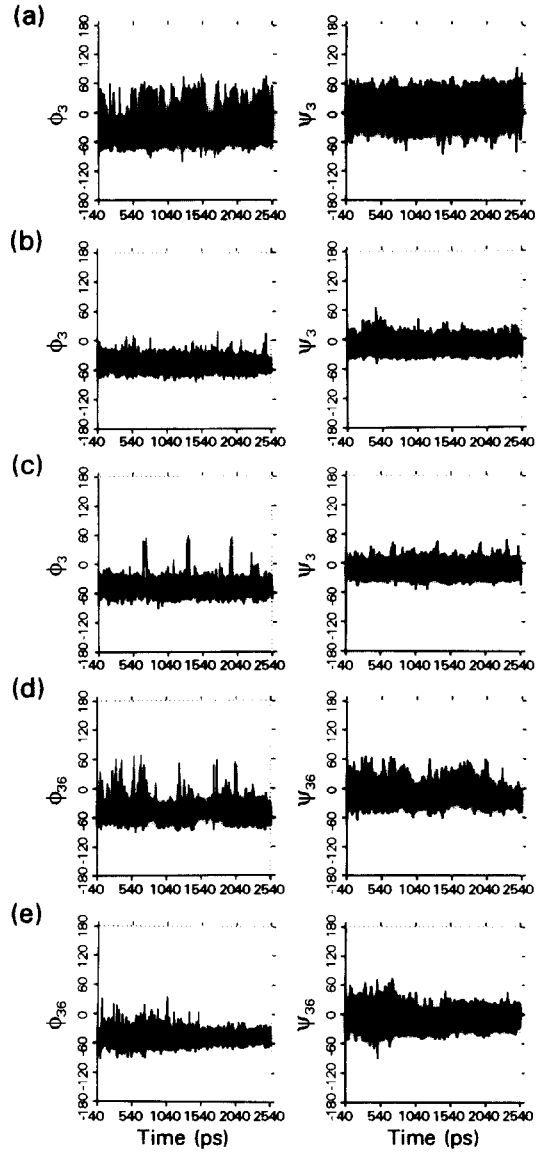

Fig. 5. Variation of the interglycosidic torsion angles around the α1,3-linkages. Torsion angle vs. time plots for Φ_3,Ψ_3 ((a), (b) and (c)) and Φ_{36},Ψ_{36} ((d) and (e)) extracted from the dynamics trajectories of M5G1 ((a) and (d)), M5G2B ((b) and (e)) and M3G3B (c). The plots for M3G1, M3G2B and M3G2 are similar to that of M5G1, M5G2B and M5G1, respectively and hence are not shown in the figure.

either Φ_3 (Fig. 6b) or Ψ_3 (Fig. 6c) or both (Fig. 6d) are also accessed occasionally during the MD simulations indicating that the addition of bis-GlcNAc does not altogether eliminate the Φ_3 and Ψ_3 values that are accessible in the absence of bis-GlcNAc. These conformations that are accessed occasionally may be important biologically since in the 2 protein-oligosaccharide crystal structures determined recently by X-ray crystallography, some interglycosidic torsion angles were found to deviate from the values preferred in free oligosaccharide [36,37].

3.3. α1,6-Linkages

As mentioned earlier, MD simulations of all the oligosaccharides were initiated with at least 2 values of χ_6 (−60°, 180°). Φ_6 fluctuates around −45°, −30° and 40° for significant lengths of time in M5G1 (Fig. 7a,b) and M5G2B (Fig. 7c,d), around −40° in M3G1 and M3G2B (Fig. 7e,f) and around −30° in M3G2 and M3G3B (Fig. 7g,h). In M3G1 and M3G2B, Φ_6 frequently accesses values close to 50° also (Fig. 7e,f). Ψ_6 in M5G1 and M5G2B favors values around 130°, 180° and −120° (Fig. 7a–d) and the changes in Ψ_6 are correlated to those in Φ_6: with χ_6 around −60°, when Φ_6 assumes a value near −60°, Ψ_6 changes to around 180° and when Φ_6 is around 60°, Ψ_6 changes to around 120°. When χ_6 is around 180°, Φ_6 and Ψ_6 assume values around −30° and −120°, respectively (Fig. 7a–d). In M3G1 and M3G2B, Ψ_6 has an average value of about 180° but it accesses values around −70° and 70° also (Fig. 7e,f). On the other hand, Ψ_6 has average values around 75° and 90° in M3G2 and M3G3B, respectively (Fig. 7g,h) and accesses values around 180° only occasionally (M3G2 — Fig. 8; M3G3B — Fig. 7h). Values close to 76° have been observed for Ψ_6 (the possibility of which was not considered while interpreting the NMR data) in the crystal structure of *Erythrina corallodendron* lectin with an *N*-linked heptasaccharide

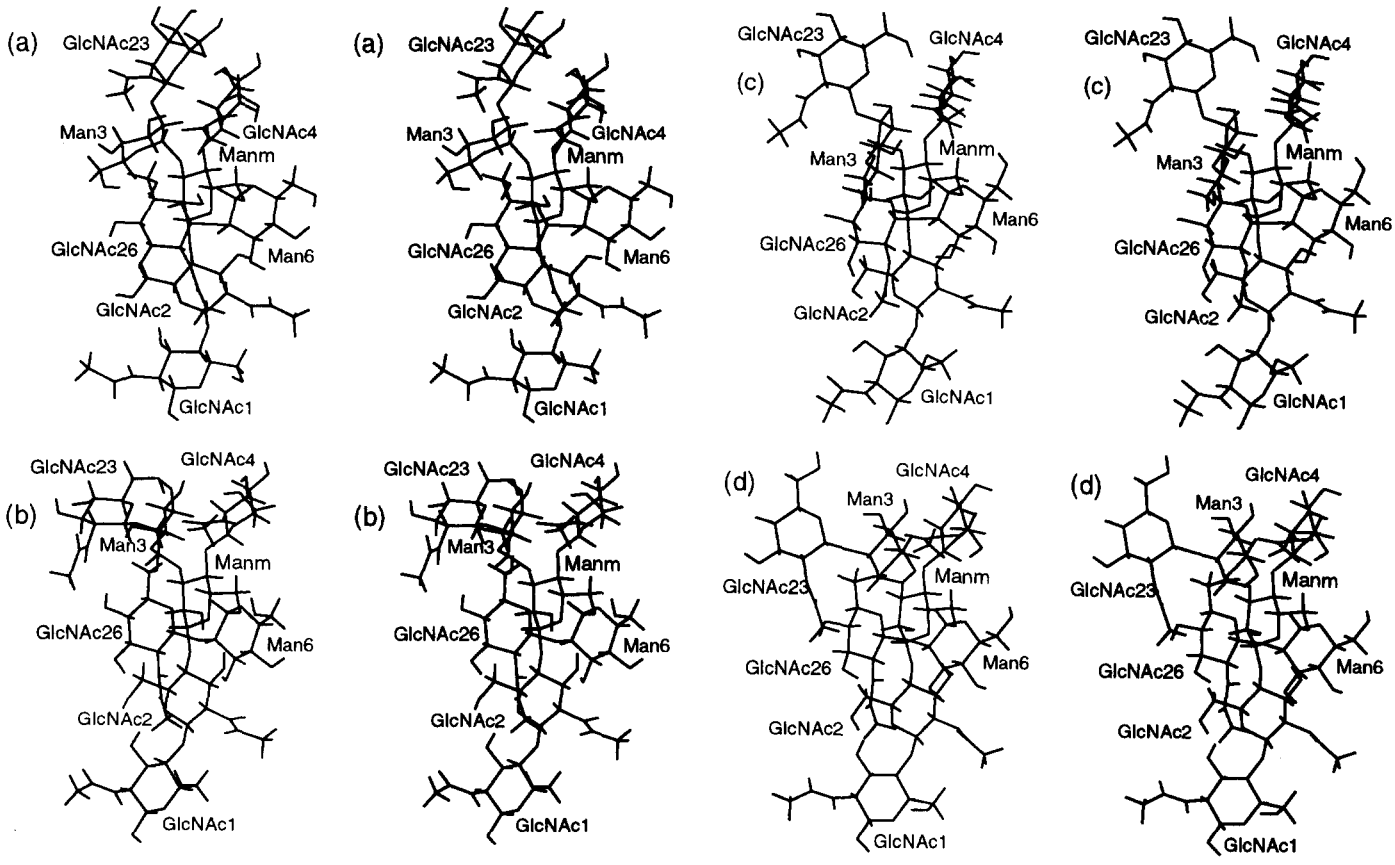

Fig. 6. Stereo diagram to show the different orientations possible for the $GlcNAc_{23}$–β1,2-Man_3 fragment relative to bis-GlcNAc ($GlcNAc_4$) in the bisecting biantennary complex oligosaccharide M3G3B. These 4 conformations, which were accessed during the MD simulations with initial Φ_6,Ψ_6-,χ_6 = −60°,130°,−60° at 2167 ps (a), 687.5 ps (b), 2501 ps (c) and 1948ps (d), were first superposed over one another with the C1, C3 and C5 atoms of Man_m as the reference points and then separated to avoid any spurious differences in the orientations. The interglycosidic torsion angles (Φ_4,Ψ_4), (Φ_3,Ψ_3) and (Φ_{23},Ψ_{23}) are (47°,14°), (−62°,−18°) and (33°,21°) in conformer (a), (43°,19°), (42°,−4°), and (39°,10°) in conformer (b), (41°,−3°), (−48°,36°) and (77°,−6°) in conformer (c) and (43°,14°), (39°,40°) and (7°,−10°) in conformer (d), respectively. The conformations (b), (c) and (d) are accessed only occassionally. Conformer (a) is the same as that in Fig. 10c.

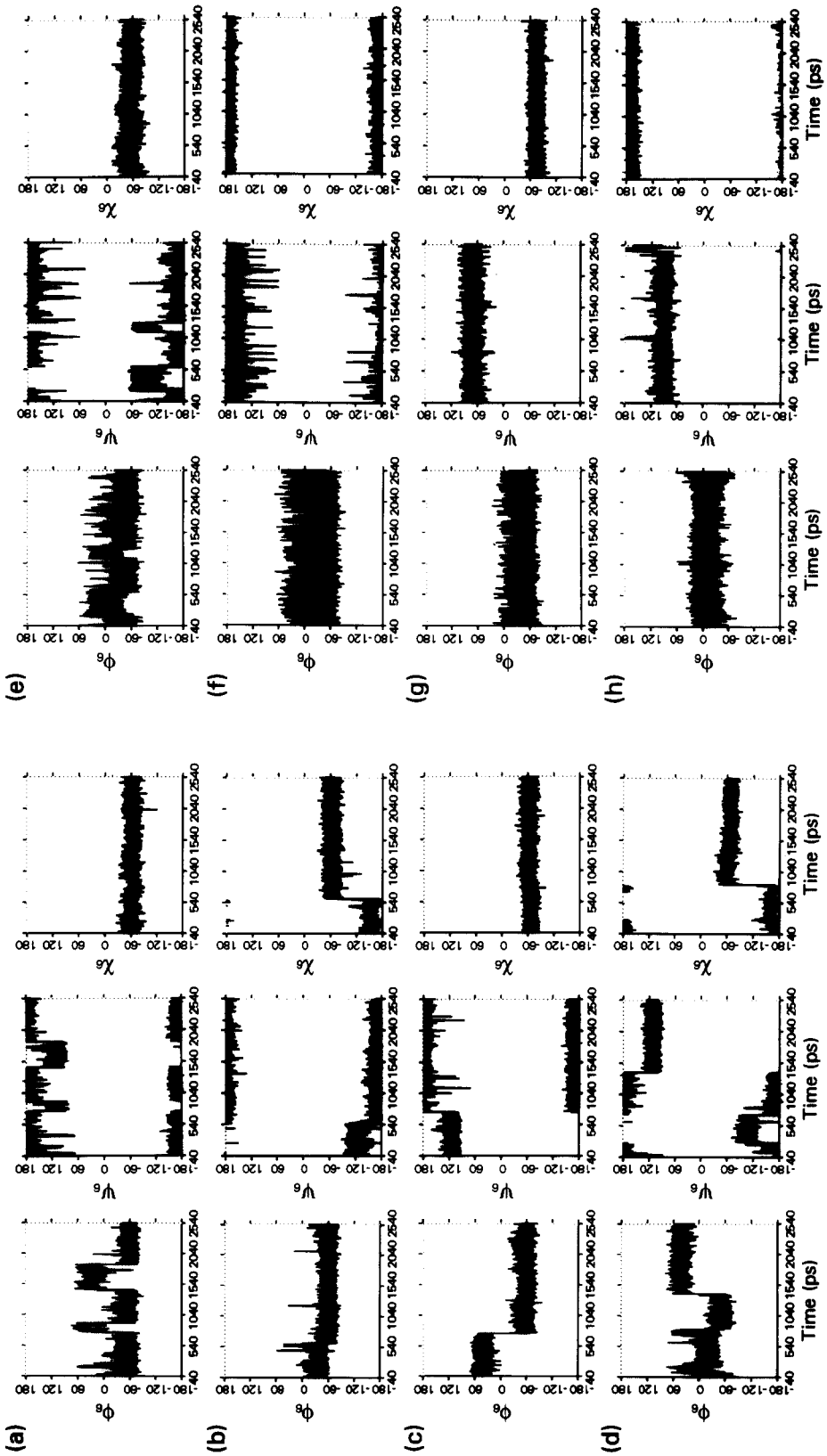

Fig. 7. Variation of the interglycosidic torsion angles around the α1,6-linkages. Torsion angle vs. time plots for Φ_6,Ψ_6,χ_6 extracted from the dynamics trajectories of M5G1 ((a) and (b)), M5G2B ((c) and (d)), M3G1 (e), M3G2B (f), M3G2 (g) and M3G3B (h). Initial values of Φ_6,Ψ_6,χ_6 are −60°,150°,−60° (a), −60°,150°,180° (b), −60°,150°,−60° (c), −60°,150°,180° (d), −60°,150°,−60° (e), −60°,180°,180° (f), −60°,150°,180° (g), −60°,130°,150° (h).

[36]. Similar observations have also been made in the MD simulations of the heptasaccharide Man-α1,6-[Man-α1,3][Xyl-β1,2]-Man-β1,4-GlcNAc-β1,4-[L-fuc-α1,3]-GlcNAc [32]. The fluctuations in Ψ_6 are dampened in M5G1, M5G2B, M3G2 and M3G3B compared to that in M3G1 and M3G2B probably because Man_6 is the terminal residue in the latter two oligosaccharides (i.e., M3G1 and M3G2B) (Fig. 7).

The fluctuations in χ_6 are more dampened than those of Φ_6 and Ψ_6 in all the oligosaccharides. In the hybrid oligosaccharides M5G1 and M5G2B, in simulations started with $\chi_6 = 180°$, transition to −60° conformation takes place after 600–800 ps (Fig. 7b,d). Concomitant to changes in χ_6, changes in the interglycosidic torsion angles Φ_6, Ψ_6 and Φ_m are also observed (to around −60°, 180°, and 60°, respectively; Figs. 3a and 7; also see Fig. 4). The orientation of the 1,6-arm is not only affected by changes in χ_6, but also by changes in Φ_6 and Ψ_6 in M5G1 (Fig. 4) and M5G2B (Fig. 9). In M3G1, χ_6 favours values around −60° irrespective of the initial values (Fig. 7e) perhaps due to the possibility of formation of a hydrogen bond between Man_6:O4 and $GlcNAc_2$:O7. Such a hydrogen bond may be weakened in presence of water as these groups prefer to form hydrogen bond with solvent. In M3G2 also, χ_6 favours values around −60° (Fig. 7g) but in some of the runs started with $\chi_6 = 180°$ transition to −60° was not observed even after 2.5 ns of simulation (data not shown). In bisected complex oligosaccharides M3G2B and M3G3B, χ_6 does not show any change from the initial value in any of the runs (Fig. 7f,h; data not shown for simulations started with $\chi_6 = -60°$) and it fluctuates around either −60° or 180° without any transition during the entire simulation period. In M3G3B, independent of the χ_6 value, i.e., whether −60° or 180°, Ψ_6 favours values around 90° and shows transitions to 180°

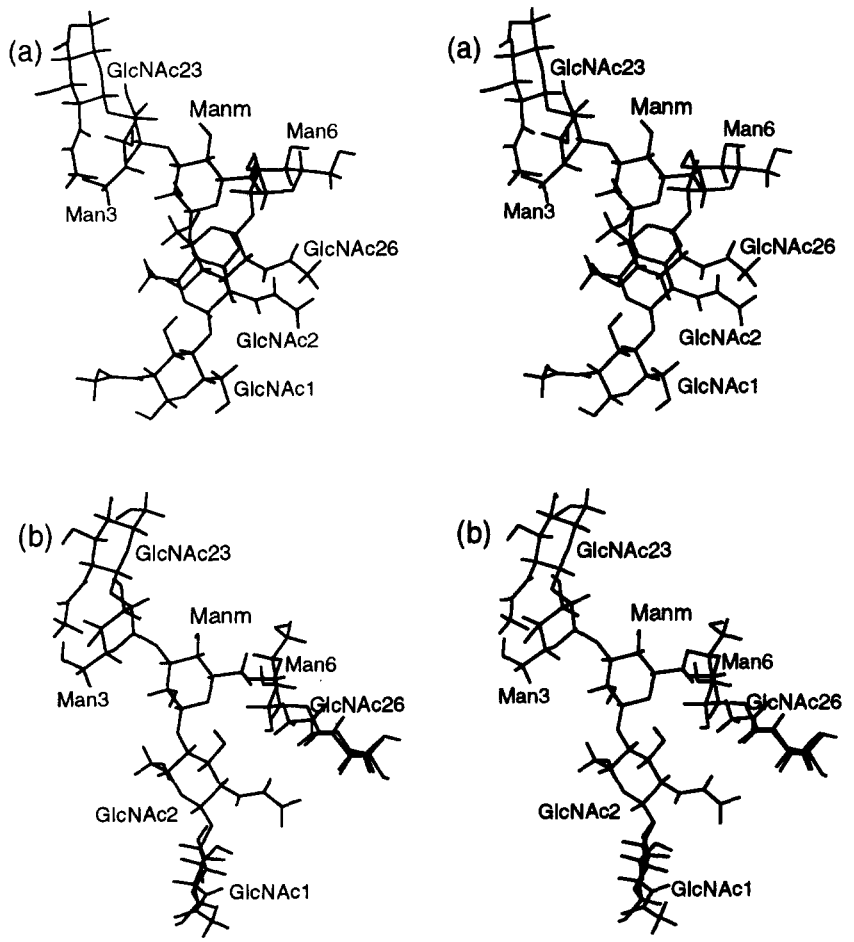

Fig. 8. Stereo diagram of 2 conformers of the biantennary complex oligosaccharide M3G2 accessed during the MD simulations to show the relative orientations of the 1,3- and the 1,6-arms. The two conformers were selected from the MD trajectories at 493 ps (a) and 755.5 ps (b) (initial Φ_6,Ψ_6, $\chi_6 = -60°,150°,180°$). The two conformers were first superimposed over each other with the C1, C3 and C5 atoms of Man_m as reference points to avoid spurious differences in the orientations. The Φ_6,Ψ_6,χ_6 and Φ_{26},Ψ_{26} values are −10°,93°,168° and 43°,29° in (a) and −7°,172°,−163° and −13°,−30° in (b). Conformer (b) with Ψ_6 around 180° is accessed rarely.

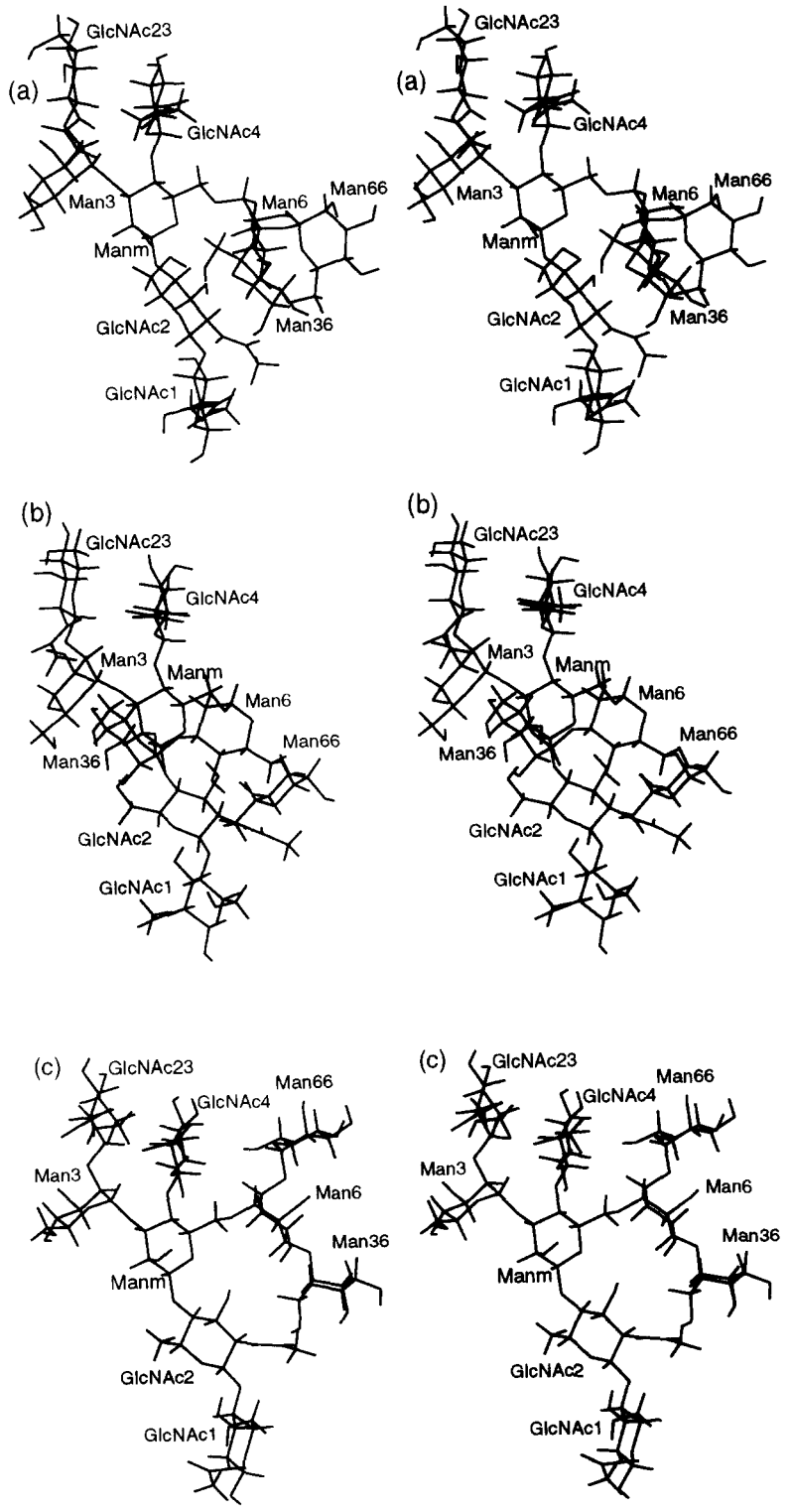

Fig. 9. Stereo diagrams of 3 conformers of the bisecting hybrid oligosaccharide M5G2B accessed during the MD simulations to show the changes in the orientation of the 1,6-arm brought about by changing χ_6 alone ((b) compared with (c)) and by changing only Φ_6 and Ψ_6 ((a) and (b) compared with (c)). The 3 conformers were accessed during the MD simulations at 1099 ps (a), 2480 ps (b) and 456 ps (c) (initial $\Phi_6,\Psi_6,\chi_6 = -60°,150°,180°$). The Φ_6,Ψ_6,χ_6 values are $-52°,-156°,-67°$ in conformer (a), $45°,116°,-75°$ in conformer (b) and $41°,-174°,180°$ in conformer (c). The conformer (c) is accessed only for a short period during the beginning of the MD simulation run. Unlike M5G1 (Fig. 4), the values of Φ_m,Ψ_m (69°,26° in (a), 56°,−5° in (b) and 69°,−11° in (c)) are in the same range in the 3 conformers of M5G2B. The 3 conformers were first superimposed over one another with the C1, C3 and C5 atoms of Man_m as reference points to avoid spurious differences in the orientations.

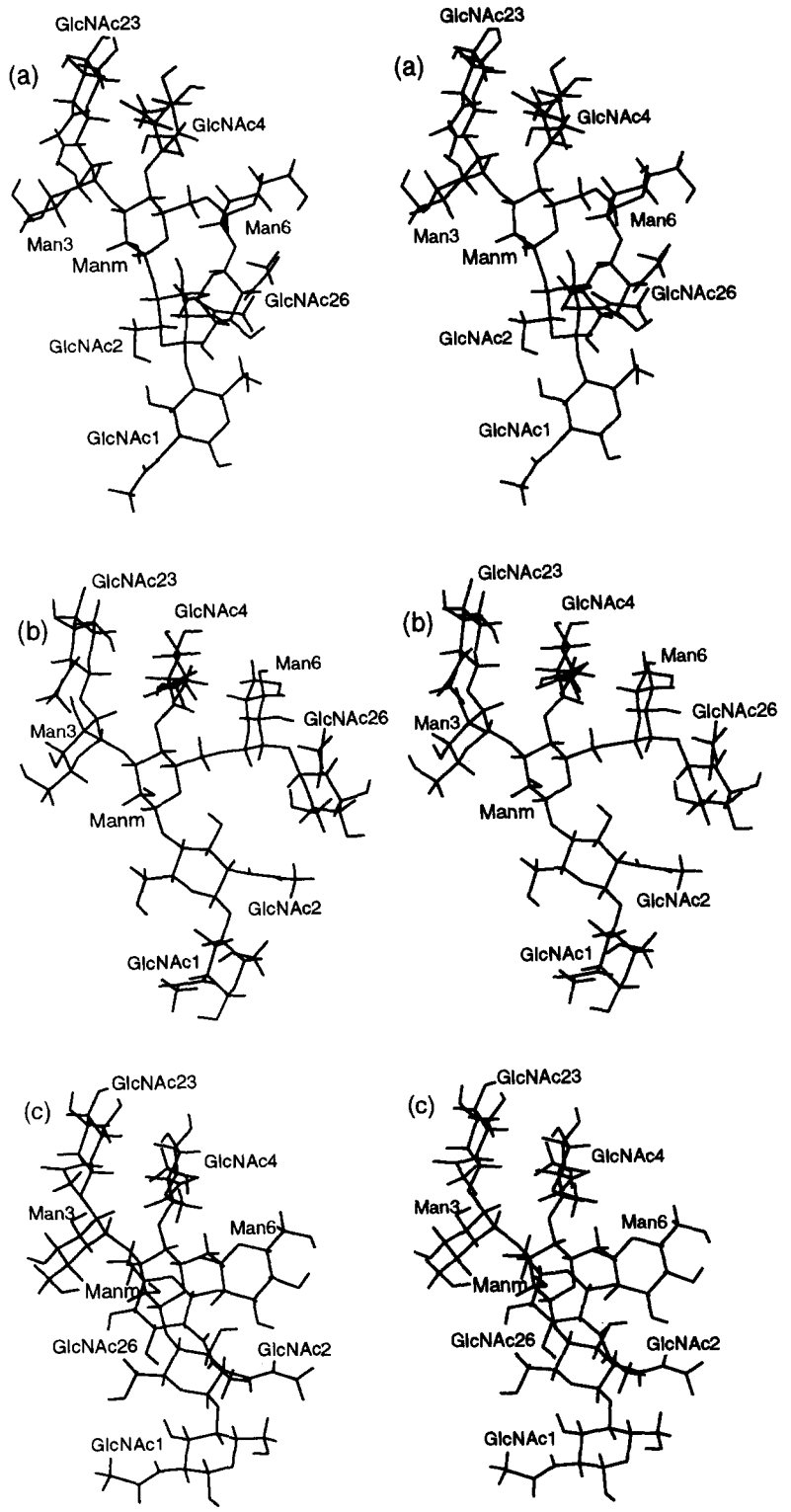

Fig. 10. Stereo diagram of 3 conformers of the bisecting biantennary complex oligosaccharide M3G3B accessed during the MD simulations to show the changes in the orientation of 1,6-arm brought about by changing χ_6 alone (conformer (a) compared with (c)) and by changing only Φ_6 and Ψ_6 alone (conformer (a) compared with (b)). The 3 conformers were accessed during the MD trajectories at 1820 ps (a) and 1054 ps (b) (initial $\Phi_6,\Psi_6,\chi_6 = -60°,130°,150°$) and 2167 ps (c) (initial $\Phi_6,\Psi_6,\chi_6 = -60°,130°,-60°$). The Φ_6,Ψ_6,χ_6 values are $-1°,101°,172°$ in conformer (a), $-61°,168°,171°$ in conformer (b) and $-25°,81°,-65°$ in conformer (c). The conformer (b) is accessed only for very short periods during the MD simulations. Notice the change in the conformation of the oligosaccharide around the $GlcNAc_{26}$–β1,2-Man_6 fragment in conformer (c) compared to that in conformers (a) and (b): the values of Φ_{26},Ψ_{26} are 35°,19° in (a), 50°,35° in (b) and 172°,28° in (c). The 3 conformers were first superimposed over each other with the C1, C3 and C5 atoms of Man_m as reference points to avoid spurious differences in the orientations. Conformer (c) is same as that in Fig. 6a.

only occasionally (once around 1050 ps and once towards the end of MD run; Fig. 7h). In these preferred conformations of M3G3B (i.e., with Ψ_6 around 90°), $GlcNAc_{26}$ is positioned close to the core residues. However, a change in Ψ_6 from around 90° to around 180° positions $GlcNAc_{26}$ away from the core residues (compare Figs. 10a, 10b with 10c). It can also be seen from Figs. 10a and 10c that the position and orientation of $GlcNAc_{26}$ relative to Man_m and $GlcNAc_2$ are different for the different values of χ_6. When χ_6 is around 180°, $GlcNAc_{26}$ is on the same side as the axial 2-OH of Man_m (Fig. 10a) whereas when χ_6 is around −60°, $GlcNAc_{26}$ is on the opposite side of the 2-OH of Man_m (Fig. 10c). A cursory look at Figs. 10a–c shows that transition of χ_6 from −60° to 180° or vice versa is possible only when Ψ_6 is around 180° (as in Fig. 10b). This perhaps explains why such a transition was not observed even when the simulations were run for 2.5 ns. If the simulations are run for even longer periods, probably the χ_6 transitions will be observed since Ψ_6 does show transitions to around 180° occasionally as mentioned earlier.

M3G2 is the product of action of GlcNAc-T II on M3G1 (Fig. 1). A comparison of the MD trajectories of M3G2 with that of M3G1 shows the effect of addition of $GlcNAc_{26}$ on the oligosaccharide. It can be seen from Figs. 3, 5, and 7 that in addition to dampening the fluctuations of Φ_{g1},Ψ_{g1}, Φ_m,Ψ_m and Φ_6,Ψ_6,χ_6, the preferred value of Ψ_6 is also affected in M3G2. In M3G1, Ψ_6 has an average value around 180° and accesses values around 75° frequently. On the other hand, Ψ_6 in M3G2 prefers a value around 75–120° and accesses values around 180° occasionally. Such a change in the preferred value of Ψ_6 causes the $GlcNAc_{26}$ to be positioned in close juxtaposition to the core chitobiose residues which explains the relatively dampened fluctuations of Φ_{g1},Ψ_{g1}, Φ_m,Ψ_m and Φ_6,Ψ_6,χ_6.

The terminal Man_{66}–α1,6-Man_6 fragment in M5G1 and M5G2B seems to favor a conformation different from that of internal Man_6–α1,6-Man_m fragment. Unlike χ_6 which favours mainly the −60° and 180° conformations, χ_{66} favours all the 3 staggered conformations, namely, 180°, −60° and 60°. During the simulation period of 2500 ps, transitions from one staggered conformation to the other have been observed (data not shown). Similar behavior has also been observed for χ_{66} in high mannose type of oligosaccharides [25]. In the χ_{66} = 60° conformation, the unfavorable syn-axial interactions (Hassel-Ottar Effect) [38] between O4 and O6 atoms of Man_6 are offset by a possible hydrogen bond between O6 and C4 hydroxyl groups (also see Ref. [39]).

3.4. β1,2-Linkages

In all the oligosaccharides, Φ_{23},Ψ_{23}, which determine the conformation around the $GlcNAc_{23}$–β1,2-Man_3 fragment, generally fluctuate around 30°,25° (data not shown). In unbisected oligosaccharides (M5G1, M3G1 and M3G2), Φ_{23} occasionally accesses values close to 180° leading to flipping of the terminal $GlcNAc_{23}$ residue. However, the presence of the bis-GlcNAc as in M5G2B, M3G2B and M3G3B not only dampens the fluctuations in Φ_{23},Ψ_{23} but also restricts the flipping of the terminal $GlcNAc_{23}$. Similar to Φ_{23},Ψ_{23}, Φ_{26},Ψ_6 also favor values around 30°,0°. In one of the simulations of M3G3B with initial Φ_6,Ψ_6,χ_6 = −60°,130°,−60°, Φ_{26} fluctuates around 180° throughout the 2.5 ns simulation period. However, in the simulations started with Φ_6,Ψ_6, χ_6 = −60°,130°,150°, Φ_{26} fluctuates around 30°. Similar observations, i.e., Φ_{26} being around 180° when χ_6 is around −60°, were also made in the MD simulations of a triantennary complex oligosaccharide which acts as the ligand for the asialoglycoprotein receptor (oligosaccharide #IV in Ref. [31]). Interestingly, the 1,6-arm is monoantennary in both these oligosaccharides (M3G3B and oligosaccharide #IV). In the unbisected complex oligosaccharide M3G2 also, Φ_{26} can assume values near 180° indicating the possibility of flipping of $GlcNAc_{26}$.

4. Discussion

4.1. Correlation with the earlier force field calculations

The conformations accessed by the individual disaccharide fragments of all the oligosaccharides are in good agreement with those reported for isolated disaccharides [40,41]. In the case of the β1,4- and β1,2-linkages, conformations corresponding to Φ around both 0–60° and 140–180° (i.e., both the low energy regions in the conformational energy map of disaccharides) are accessed in the MD simulations. On the other hand, for the α1,3-linkage, only those conformations corresponding to Φ or Ψ ranging from −60° to 60° are accessed. Conformations corresponding to Ψ around 180° were accessed in only one of the runs of M3G2 (data not shown) and those corresponding to Φ around 180° were not accessed in any of the simulations. Similar observations have been made from the NMR-restrained molecular dynamics [42] and monte carlo [43] studies on the conformation of Man-α1,3-Man-α1,-OCH_3. In the NMR-MD study, the AMBER-derived carbohydrates force field of Homans was used [44] and it was found that the conformation corresponding to Φ,Ψ = 30°,−150° was observed only in simulations that considered solvent molecules explicitly but not in the in vacuo simulations. Interestingly, in the in vacuo simulations starting from this latter conformation, the disaccharide exits rapidly from this minimum even in the absence of any NOE constraints [42]. The monte carlo simulations were done using the HSEA force field at both 300 and 600 K. In neither of these simulations, conformations with either Φ or Ψ around 180° were accessed [43].

From conformational analysis of hybrid and complex oligosaccharides using NMR spectroscopy, it was sug-

gested that χ_6 prefers values around −60° in hybrid and unbisected biantennary complex oligosaccharides [45, 46]. However, another NMR study concluded that χ_6 in these oligosaccharides prefer both −60° and 180° [47]. But for χ_6 in bisected complex oligosaccharides, both these NMR studies suggest 180°. In the simulations of hybrid oligosaccharides (M5G1 and M5G2B), χ_6 changes to −60° after about 600–800 ps when the simulations are started with χ_6 around 180°. In the present simulations of unbisected complex oligosaccharides, χ_6 prefers −60° except in a few runs of M3G2 with initial χ_6 around 180°. In the bisected complex oligosaccharides, there is no change in the initial value of χ_6 throughout the 2.5 ns simulation period.

The preferred conformations of M3G2 and M3G3B have been studied by empirical potential energy calculations [30] (S-2a and S-2b in Ref. [30] are the same as M3G2 and M3G3B, respectively) and all the minimum energy conformations reported from this study are accessed in the present MD simulations. From NMR and molecular dynamics simulations of M3G2 and M3G3B, bis-GlcNAc was found to affect only the core α1,3- and α1,6-linkages and that bis-GlcNAc has a direct steric influence over Φ_3 and Ψ_3 [33]. These are in agreement with the present simulations where the fluctuations of β1,4- and the β1,2-linkages are similar in both M3G2 and M3G3B. However, in these two oligosaccharides, the conformations of the α1,3- and the α1,6-linkages are different as discussed in Results.

A new molecular mechanical force field was derived for the conformational analysis of oligosaccharides starting from AMBER force field and, using this force field, it was found that the torsion angles corresponding to Φ_m,Ψ_m in both the Man-β1,4-GlcNAc disaccharide and the Man-α1,3-Man-β1,4-GlcNAc trisaccharide are restricted to the region around the global minimum (52°,1°) [44]. MD simulations of the above mentioned di- and trisaccharides both in vacuo (dielectric constant = 80) and with explicit solvent showed that the interglycosidic torsion angles fluctuate only around the global minimum conformation. However, the fluctuations were dampened in the presence of solvent molecules. These results show that the conformations accessed for the Man_m-β1,4-$GlcNAc_2$ fragment in the oligosaccharides studied here (Fig. 1) with the CVFF force field are similar to those accessed in the Man-β1,4-GlcNAc disaccharide and the Man-α1,3-Man-β1,4-GlcNAc trisaccharide with Homans' force field. These results also show that the explicit inclusion of solvent in the simulations will have only a dampening effect and does not cause the oligosaccharide to access any new conformations.

4.2. Correlation with biochemical data

Some of the glycosyltransferases have been shown to exhibit branch specificity. For example, the rate of transfer of galactose by rat liver Golgi β-1,4-galactosyltransferase to the GlcNAc on the 1,3-arm ($GlcNAc_{23}$) of the biantennary complex oligosaccharide M3G2 was shown to be at least 5 times faster than to the GlcNAc on the 1,6-arm ($GlcNAc_{26}$) [48]. The transfer of galactose by bovine colostrum and calf thymus membrane β-1,4-galactosyltransferases to the biantennary substrate GlcNAc-β1,2-Man-α1,3[GlcNAc-β1,2-Man-α1,6]-Man-β1,4-GlcNAc (i.e., M3G2 without $GlcNAc_{gl}$) [49] and by swine mesentary lymph node enzyme to the biantennary oligosaccharide of IgG [50] also led to similar conclusions. This branch specificity has been attributed to the greater accessibility of the GlcNAc on the 1,3-arm ($GlcNAc_{23}$) compared to the GlcNAc on the 1,6-arm ($GlcNAc_{26}$). Two of the typical conformers of M3G2 that are accessed during the MD simulations are shown in Fig. 8. Of the two, one conformer (Fig. 8a) is more frequently accessed than the other (Fig. 8b). In both the conformers, the GlcNAc on the 1,3-arm ($GlcNAc_{23}$) is placed away from the core and is more accessible than the GlcNAc on the 1,6-arm ($GlcNAc_{26}$). This is in agreement with the suggestions made by earlier workers [48–50] to explain the branch specificity of β-1,4-galactosyltransferase.

During the biosynthesis of hybrid and complex type oligosaccharides, the addition of bis-GlcNAc catalyzed by GlcNAc-T III has been shown to inhibit the subsequent action of some of the enzymes like mannosidase II, GlcNAc-T II, GlcNAc-T IV and GlcNAc-T V [51,52]. There have been conflicting views about the role played by bis-GlcNAc in the inhibition of these enzymes. Based on a detailed investigation of the action of different glycosyltransferases on a variety of oligosaccharide substrates [53] combined with the NMR studies on the conformation of these substrates [35], it was proposed that the bis-GlcNAc sterically interferes with the binding of oligosaccharide substrates to the enzymes. On the other hand, Homans et al., [34] from NMR and MNDO calculations of several Asn-linked oligosaccharides, concluded that the presence of bis-GlcNAc affects the conformational transitions of the α1,3-arm and explained the inability of mannosidase II and GlcNAc-Ts to act on bisected substrates as due to such a restriction of the α1,3-arm. The present MD simulations show that in the presence of bis-GlcNAc, those conformations where either Φ_3 or Ψ_3 are greater than 0 are rarely accessed indicating that such conformations are not stereochemically eliminated. Recent studies have shown that such less favored conformations of oligosaccharides may indeed be the conformations adopted by these molecules in the protein-bound form [17]. In view of this, it seems more plausible that the inhibition of glycosyltransferases and mannosidases by bis-GlcNAc is probably due to steric interference rather than exclusion of any conformations of the core α1,3- and α1,6-linkages. In fact, computer modeling studies on the

binding of bisected and unbisected oligosaccharides to the plant lectin concanavalin A showed that bis-GlcNAc significantly affects the accessibility of the residues which bind to ConA and thereby reduces their binding affinity to the lectin [54].

Acknowledgements

The authors acknowledge the National Cancer Institute for the allocation of computing time and staff support at the Frederick Biomedical Supercomputing Center of the Frederick Cancer Research and Development Center.

References

[1] Kornfeld R and Kornfeld S. *Annu Rev Biochem* 1985; 54: 631.
[2] Moremen KW, Trimble RB and Herscovics A. *Glycobiology* 1994; 4: 113.
[3] Schachter H. *Glycobiology* 1991; 1: 453.
[4] Van den Eijnden DH and Joziasse DH. *Curr Opin Struct Biol* 1993; 3: 711.
[5] Kobata A and Takasaki S. *Cell surface carbohydrates and cell development* (Ed. M Fukuda), CRC Press, Boca Raton, 1992; 1.
[6] Narasimhan S, Stanley P and Schachter H. *J Biol Chem* 1977; 252: 3926.
[7] Li E and Kornfeld S. *J Biol Chem* 1978; 253: 6426.
[8] Cummings RD, Trowbridge IS and Kornfeld S. *J Biol Chem* 1982; 257: 13421.
[9] Campbell C and Stanley P. *J Biol Chem* 1984; 261: 13370.
[10] Yamashita K, Tachibana Y, Ohkura T and Kobata A. *J Biol Chem* 1985; 260: 3963.
[11] Chaney W and Stanley P. *J Biol Chem* 1986; 261: 10551.
[12] Dennis JW, Laferte S, Waghorne C, Breitman M and Kerbel RS. *Science* 1987; 236: 582.
[13] Fukuda MN, Dell A and Scartezzini P. *J Biol Chem* 1987; 262: 7195.
[14] Pierce M, Arango J, Tahir SH and Hindsgaul O. *Biochem Biophys Res Comm* 1987; 146: 679.
[15] Yousefi S, Higgins E, Daoling Z, Pollex-Krueger A, Hindsgaul O and Dennis JW. *J Biol Chem* 1991; 266: 1772.
[16] Muramatsu T. *Glycobiology* 1993; 3: 294.
[17] Homans SW. *Glycobiology* 1993; 3: 551.
[18] Carver JP. *Curr Opin Struct Biol* 1991; 1: 716.
[19] Paulsen H, Peters T, Sinnwell V, Lebuhn R and Meyer B. *Liebigs Ann Chem* 1985; 489.
[20] Breg J, Kroon-Batenburg LMJ, Strecker G, Montreuil J and Vliegenthart JFG. *Eur J Biochem* 1989; 178: 727.
[21] Bouwstra JB, Spoelstra EC, De Waard P, Leeflang BR, Kamerling JP and Vliegenthart JFG. *Eur J Biochem* 1990; 190: 113.
[22] Poppe L, Stuike-Prill R, Meyer B and Van Halbeek H. *J Biomol NMR* 1992; 2: 109.
[23] Edge CJ, Singh UC, Bazzo R, Taylor GL, Dwek RA and Rademacher, TW. *Biochemistry* 1990; 29: 1971.
[24] Mazurier J, Dauchez M, Vergoten G, Montreuil J and Spik G. *Glycoconj J* 1991; 8: 390.
[25] Balaji PV, Qasba PK and Rao VSR. *Glycobiology* 1994; 4: 497.
[26] Qasba PK, Balaji PV and Rao VSR. *J Mol Struct* 1996; in press.
[27] Satyanarayana BK and Rao VSR. *Biopolymers* 1971; 10: 1605; erratum in 11: 1115.
[28] Satyanarayana BK and Rao VSR. *Biopolymers* 1972; 11: 1379.
[29] Biswas M, Sekharudu YC and Rao VSR. *Carbohydr Res* 1987; 160: 151.
[30] Biswas M, Sekharudu YC and Rao VSR. *Int J Biol Macromol* 1986; 8: 2.
[31] Balaji PV, Qasba PK and Rao VSR. *Biochemistry* 1993; 30: 12599.
[32] Qasba PK, Balaji PV and Rao VSR. *Glycobiology* 1994; 4: 805.
[33] Rutherford TJ and Homans SW. *Biochemistry* 1994; 33: 9606.
[34] Homans SW, Dwek RA and Rademacher TW. *Biochemistry* 1987; 26: 6553.
[35] Brisson J-R and Carver JP. *Biochemistry* 1983; 22: 3671.
[36] Shaanan B, Lis H and Sharon N. *Science* 1991; 254: 862.
[37] Bourne Y, Rouge P and Cambillau C. *J Biol Chem* 1992; 267: 197.
[38] Hassel O and Ottar B. *Acta Chem Scand* 1947; 1: 929.
[39] Jeffrey GA. *Acta Cryst* 1990; B46: 89.
[40] Imberty A, Gerber S, Tran V and Perez S. *Glycoconj J* 1990; 7: 27.
[41] Imberty A, Delage M-M, Bourne Y, Cambillau C and Perez S. *Glycoconj J* 1991; 8: 456.
[42] Rutherford TJ, Partridge J, Weller CT and Homans SW. *Biochemistry* 1993; 32: 12715.
[43] Peters T, Meyer B, Stuike-Prill R, Somorjai R and Brisson J-R. *Carbohydr Res* 1993; 238: 49.
[44] Homans SW. *Biochemistry* 1990; 29: 9110.
[45] Brisson J-R and Carver JP. *Biochemistry* 1983; 22: 3680.
[46] Cumming DA and Carver JP. *Biochemistry* 1987; 26: 6676.
[47] Homans SW, Dwek RA, Boyd J, Mahmoudian M, Richards WG and Rademacher TW. *Biochemistry* 1986; 25: 6342.
[48] Paquet MR, Narasimhan S, Schachter H and Moscarello MA. *J Biol Chem* 1984; 259: 4716.
[49] Blanken WM, Van Vliet A and Van den Eijnden DH. *J Biol Chem* 1984; 259: 15131.
[50] Rao AK and Mendicino J. *Biochemistry* 1978; 17: 5632.
[51] Moremen KW and Touster O. *Protein transfer and organelle biogenesis* (Eds. RC Das and PW Robbins), Academic Press, Orlando, 1988; 209.
[52] Brockhausen I, Narasimhan S and Schachter H. *Biochimie* 1988; 70: 152.
[53] Schachter H, Narasimhan S, Gleeson P and Vella G. *Can J Biochem Cell Biol* 1983; 61: 1049.
[54] Sekharudu YC, Biswas M and Rao VSR. *Int J Biol Macromol* 1986; 8: 9.